Proceedings of Meetings on Acoustics

Volume 19, 2013 http://acousticalsociety.org/

ICA 2013 Montreal
Montreal, Canada
2 - 7 June 2013

Psychological and Physiological Acoustics
Session 3aPP: Auditory Physiology and Modeling (Poster Session)

3aPP22. A physiology-based auditory model elucidating the function of the cochlear amplifier and related phenomena. Part II: Model parameters and simulations.

Sebastian Becker* and Herbert Hudde

***Corresponding author's address: Ruhr University Bochum, Inst. of Communication Acoustics, Building ID 2/231 Ruhr-Universität Bochum, Bochum, 44780, NRW, Germany, sebastian.becker-2@rub.de**

In this second of two associated papers the properties of the physiology-based auditory model are investigated. This includes finding of appropriate parameters and simulating various responses. In the end the model is intended to reproduce the human ear, hence human data is used for fitting. Only the trend of active tuning curves is based on chinchilla measurements, as human data is not available. To achieve such tuning curves the cochlea amplifier feeds energy into the system basal to the characteristic place, resulting in a locally restricted negative real part of the basilar membrane impedance. Realistic level dependent tuning curves show a reasonable input-output function and a maximum cochlear gain of 55 dB. The growth of distortion product otoacoustic emissions is consistent with measurements and shows a slope of 0.5dB/dB. The physiology-based model approach shows the origin of the distortion products within the overlap region of the stimuli and elucidates the propagation within cochlea. As reflections are a dominant factor in the generation of transient evoked otoacoustic emissions, parameters need a certain degree of roughness to achieve results corresponding to measurements. In spite of its simplicity the model is able to reproduce a variety of cochlea results with one parameter set.

Published by the Acoustical Society of America through the American Institute of Physics

 [DOI: 10.1121/1.4799318]
Received 18 Jan 2013; published 2 Jun 2013

1. INTRODUCTION

The cochlea is an essential component of the peripheral ear. Understanding the physiological mechanisms leading to the cochlea amplifier and its related effects or the loss of the very same, is of major interest when understanding human perception.

In the first of two associated papers [1] we propose a physiology based auditory model (PhyBAM). In this second paper the focus lies on the tuning process and results of our model approach, as only a model fitted to reproduce measured data is of further use. The basic idea is to have a simple human model consisting only of the yet to be determined relevant components. To identify the components a constant interplay of model tuning and enhancement is necessary, as parametrization is not a simple optimization problem. It is required to alter the model and adjust its parameters to reproduce a diversity of measured results.

A challenge in modeling the human auditory system is the incomplete data set, as physical data like the tuning sharpening, amplification and tuning curves along the basilar membrane are well-known for other mammals except humans. However a huge set of otoacoustic emissions are available for humans, that are suited to verify the model structure and tuning. There are some fundamental effects that are not the result of a simple parameter fitting, but a direct consequence of the modeled structure. A distinct negative real part of the basilar membrane impedance is predicted by de Boer et al. [2] illustrating that a simple undamped resonator cannot describe the cochlea amplifier. Shera [3] showed that the basilar membrane resonance is nearly level independent.

2. PARAMETER FINDING AND MODEL DESCRIPTIONS

When a fairly advanced human model is present, otoacoustic emissions (OAE) are ideal to study the cochlea and to finalize its parameters for humans. However, since OAE require the simultaneous and correct simulation of effects like cochlear compression, reflections and non-linear properties, physiological data such as level-dependent tuning curves are more suited in the process of model finding and intermediate tuning. Tuning curves can only be measured invasively, so no human data are available. Still these data are so characteristic that animal data among a majority of human data is used to reproduce the low-level behavior. Animal data is used to verify the approximate trends within the cochlea, like the general progression of tuning curves along the cochlea for different frequencies. In the end the model is verified utilizing OAE.

The modeled basilar membrane has a length of 35 mm and grows in width linear from base to apex from 100 to 500 μm. The mechanical coating is assumed to be constant across the cochlea and the resonance frequency of the basilar membrane resonators (Z_{BM}) are derived from auditory filters as noted by Moore [4] ranging from 40 Hz to 16 kHz. The quality-factor is fixed with $Q_{BM} = 2$.

The outer hair cell (OHC) motion transduction is considered equal to those of inner hair cells (IHC), therefore the model of Shamma et al. [5] is the basis for the OHC model. There are several non-linearities that can be taken into account, here we only consider the time variant conductance and neglect all other sources of non-linearities as the non-linear characteristic of the conductance is supposed to be the main origin of introduced harmonics [6].

The Corti resonator describes the oscillation mode of the organ of Corti when excited via the OHC. Only excitation located basal to the characteristic place shows reasonable results, therefore the resonance frequency of a corresponding Corti resonator is lower in comparison to the basilar membrane resonator at the same place by the factor R_f. Its parameters (friction $w_{CR,mech}$, compliance $n_{CR,mech}$) are defined via a quality factor Q_{CR} and the resonance frequency f_{CR}. The mass $m_{CR,mech}$ is set equal to the mechanical mass of a BM section.

In anticipation of the fitting process described in section 3.1, figure 1 shows the final parameters along the basilar membrane. The model shows no relevant activity towards the apical end, as no significant amplification is known for those regions [7] and a stable model requires a less active amplifier at the apex [8].

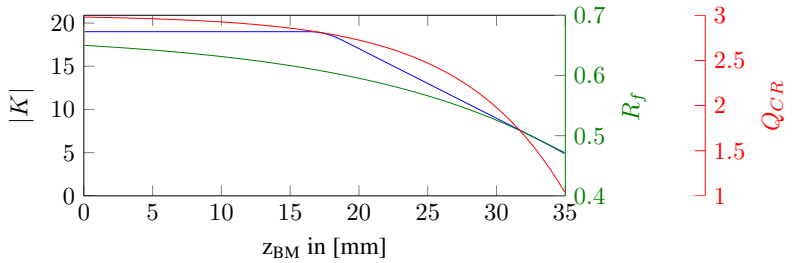

Fig. 1. The place dependent cochlea amplifier parameters.

A major problem when modeling the described electrical processes is the membrane capacitance C_m, hence together with the total conductance it is a low-pass filter with a low roll-off frequency, preventing any significant amplification for frequencies above. This effect is known as the *RC time constant problem* [9]. There are several proposed counter mechanisms like a counteracting viscous drag in the spacing between the tectorial membrane and the reticular laminar [10] or fast potassium currents [11]. Especially the latter shows that a significant bandwidth enhancement is possible, compensating the effects of the membrane capacitance in the frequency region of interest. To keep the model as simple as possible we avoid to model all the mentioned counter acting effects explicitly and neglect the membrane capacitance ($C_m = 0$). In addition no reasonable results could be achieved with an uncompensated membrane capacitance.

The coupled system was solved in time-domain using the Newmark-method and parameters equal to the trapezoidal rule with a computational sampling frequency of 400 kHz.

3. Model evaluation

In order to verify the model approach the most significant fundamental effects of the healthy cochlea are analyzed. In particular, the active tuning curves with a compression of at least 50dB, related low-level tuning sharpening and shift in characteristic place have to be achieved along with the level depending transition to the passive high-level behavior.

3.1. Low level tuning curves

Figure 2 shows the envelope of basilar membrane velocity v_{BM} normalized to the velocity at entrance of the upper channel $v_{U,0}$ across the uncoiled cochlea from base (0 mm) to apex (35 mm) . For the passive model (dashed) the system is highly damped, therefore the maximum of the envelope is in front of the characteristic place marked as a vertical line. In contrast the active model (solid) shows a significant amplification of 55 dB of the traveling wave. The rising edge of ~ 12 dB/mm shows a sharper low level tuning supporting the frequency selectivity of the cochlea for low levels. The traveling wave shows a broad and tall peak. This is contrary to the behavior of a simple undamped series resonator that is sometimes proposed. The active model shows a small damping of the traveling wave before amplification of about 4 dB.

Figure 3 shows the sensitivity plotted against the frequency for several places of the cochlea. In the model approach a constant amplification for all places was assumed, hence all tuning curves would have the same peak height. Measured chinchilla data [7] show two significant effects, on the one hand frequencies at the base show a reduced amplification. On the other hand a significant decrease in amplification and resonance shift is observed for apical frequencies, indicating a declining cochlear amplification. The first effect is already considered in our model due to the implied method of operation, as the active zone needs some space to enhance the traveling wave. The second effect is reproduced with a decrease in the excitation of the outer hair cell model with a reducing factor K and a reduction of the frequency shift R_f. Adjusting solely these parameters leads to the desired distribution of amplitudes, but all tuning curves still show the same steep slope just with a decreasing peak. To achieve the measured smoother progression for the low frequencies the Q-factor Q_{CR} has to be decreased additionally. The combined modification and broadening of excitation leads to the desired distribution and slope of the tuning curves. Figure 1 shows the resulting variation of the parameters from base to apex. The general trend of the tuning curves is fitted against data of Temchin et al. [7], as active data of humans is not available.

3.2. The active basilar membrane impedance

The actively altered basilar membrane impedance illustrates the impact of the cochlear amplifier approach and therefore shows the origin of the active tuning curves. Figure 4 shows the overall basilar membrane impedance in the middle of the cochlea corresponding to the tuning curve shown in figure 2. In contrast to the passive model (dashed) that shows the expected impedance of an acoustical series resonator, the active model (solid) shows a distinct negative real part in a small region before the characteristic place (vertical line). The imaginary part is reduced too, leading to an enhanced stiffness in this region, explaining the lower tuning curves before amplification in figure 2 at the basal end.

The method of operation becomes more clear by decomposition of the actively altered basilar membrane impedance and examination of the derived components.

$$\tilde{Z}_{BM} = Z_{BM} - \frac{p_{BM0}}{q_{BM}} = Z_{BM} - Z_{act} = Z_{BM} \cdot f_{act} \tag{1}$$

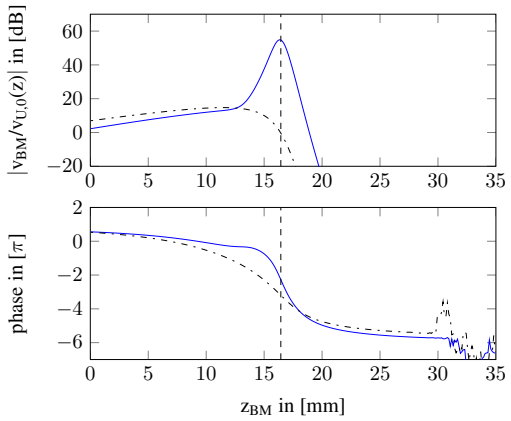

Fig. 2. Resulting tuning curves for the active (solid) and passive (dashed) model for a stimulus frequency of 2 kHz.

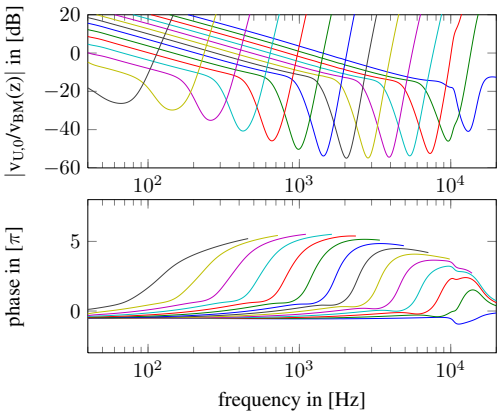

Fig. 3. Tuning curves for a set of frequencies fitted to match the overall trend of measured data of Temchin et al. [7].

Formula (1) shows the overall basilar membrane impedance decomposed into a passive and an active impedance. The additional component Z_{act} is the result of the additional force coupled into the basilar membrane by the Corti mode. The Corti resonator- and basilar membrane velocity are superimposed via the pressure source p_{BM0}. The passive impedance Z_{BM} is multiplied by an complex factor f_{act}. The components are shown in figure 5 for a frequency with a characteristic place in the middle of the cochlea. The major effect of the active factor on the passive impedance is a phase shift in a small area right before the characteristic place. Right away on the onset of the enhanced damping of the passive basilar membrane the phase shifts above $-\pi/2$, resulting in an distinct local undamping of the system. The quality factor of the Corti resonator determines the width, its resonance shift relative to the basilar membrane determines the position of the amplification. The slight shift in the resonance frequency showed to be nearly level independent and is consistent with findings by Shera [3].

The complex factor is essential. The first model approach used a mechanical series resonator to represent the Corti mode, resulting in a Z_{act} that is not proportional to Z_{BM}. This shares similarities to the approach of Neely et al. [12] and leads to a distinct restricted damping before amplification that is not in agreement with measurements. In consequence the model structure was altered to the presented mechanical parallel resonator and the resulting vibrations superimposed.

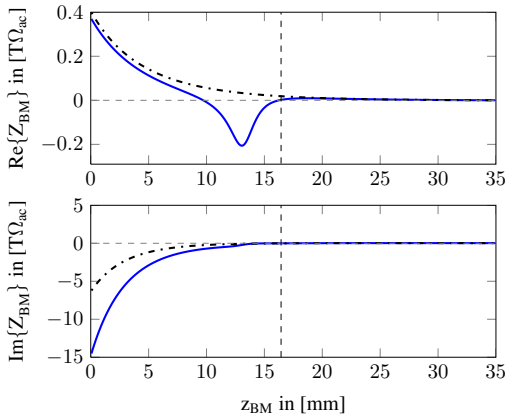

Fig. 4. Real and imaginary part of the basilar membrane impedance, for the active (solid) and passive (dashed) model. The active impedance shows a negative real part for about 5 mm right before the characteristic place.

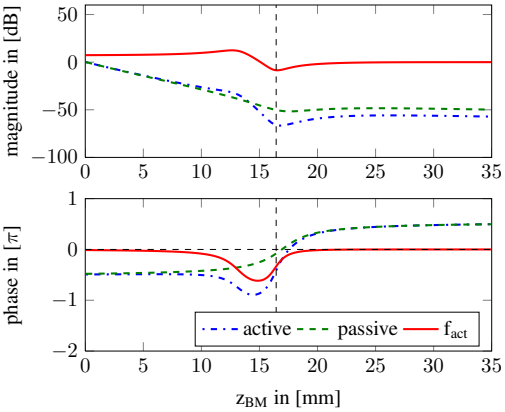

Fig. 5. Magnitude and phase components of the active basilar membrane impedance. To obtain the same range the components are normalized and shown in arbitrary units.

3.3. Level dependent tuning curves and I/O characteristic

The low-level model is linear. But with rising excitation level the OHC saturate, leading to non-linear effects. To analyze the level dependent behavior of our approach, the model is excited with 2 kHz pure tone stimuli of different excitation level. The levels at the ear canal range from 0 to 140 dB SPL in steps of 10 dB. The envelope is computed in time domain from the maximum basilar membrane velocity. Therefor the frequency dependent settling time t_s has to be considered, which is proportional to these of passive basilar membrane resonators $t_s \sim Q_{BM}/f$, for the active system it about 30 to 70 times longer.

In principle, the model is able to achieve a gain of 65dB. This setting is robust and stable for low levels, yet its response shown in figure 6 is heavily disturbed for intermediate levels. This is due to introduced additional frequencies by the non-linear OHC characteristics and the amplification of even small signal components. These distortions could only be reduced with a decreased gain of 55 dB. It becomes obvious that the achievable amplification is limited by the introduced distortions and not by the system stability for low-levels.

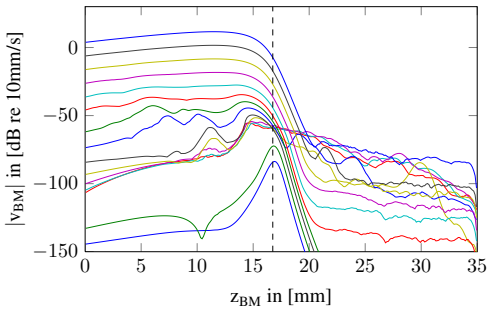

Fig. 6. Distorted level dependent tuning curves of the basilar membrane velocity plotted along the cochlea from base (0 mm) to apex (35 mm) for a 2 kHz pure tone for different excitation levels ranging from 0 to 140 dB SPL.

Figure 7 shows the resulting tuning curves plotted against the length of the cochlea for the reduced gain of 55dB. For small amplitudes the model shows the discussed active tuning curves. The characteristic place (CP) is identified as the maximum of the traveling wave; with rising amplitude the CP shifts to the basal end. In distance from the CP a linear growth can be observed due to the locally restricted operation of the cochlea amplifier. In consequence of the OHC saturation there is a linear growth for large amplitudes. On the rising slope there are reflections depending on the saturation and amplification.

For a better representation of the non-linear behavior the input-output function of the basilar membrane is well suited, as it is possible to see the resulting compression and saturation. For 2 kHz pure tone stimuli the maximum velocity for each excitation level is evaluated at a single place, the characteristic place determined for 0 dB SPL. Figure 8 shows the input-output function. As both the active and the high-level model are linear the function shows a linear growth for low-levels (0 - 20 dB SPL) that saturates for intermediate levels (30 - 90 dB SPL) and is linear again for a fully saturated cochlea amplifier (> 100 dB SPL). The I/O function is influenced by several model parameters: The compression is equal to the achieved amplification, the slope of the saturation is governed by the OHC characteristic and the position of the saturation can be controlled with K and K_{OHC} as with these the dynamic range of the OHC can be adjusted.

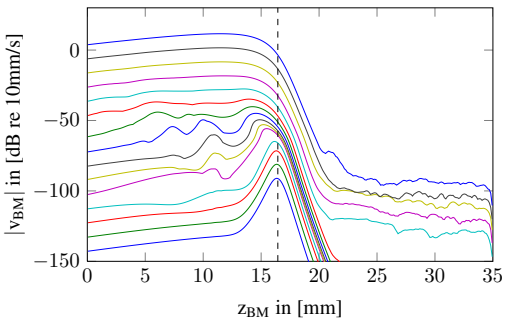

Fig. 7. Level dependent tuning curves of the basilar membrane velocity plotted along the cochlea from base (0 mm) to apex (35 mm) for a 2 kHz pure tone for different excitation levels ranging from 0 to 140 dB SPL.

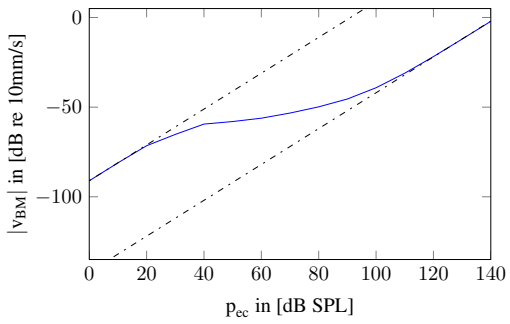

Fig. 8. Input-output function of the basilar membrane for a 2 kHz pure tone as a function of the ear canal sound pressure and an amplification of 55 dB. The low- and high-level growth is linear indicated by the dashed lines.

4. Simulation of otoacoustic emissions

The model is at an early stage for otoacoustic emissions (OAE) simulation, as it is only tuned to fulfill tuning curves. OAE include more effects as the non-linear interaction and all basilar membrane parameters have to be exact to reproduce human data. No further tuning of the model for these simulations was performed, therefore it is unlikely to achieve realistic results, but hints how to tune and enhance the model. We analyze two evoked OAE types. For the distortion product otoacoustic emissions the I/O function must be correct along with the excited area of the cochlea and amplification, due to the non-linear interaction of the occurring stimuli. Transient evoked otoacoustic emissions are more demanding, as additionally the temporal properties have to be equal to these of humans.

4.1. Distortion product otoacoustic emissions

Distortion product otoacoustic emissions (DPOAE) are generated within the cochlea because of the interaction of two stimuli with differing frequencies f_1 and f_2. Due to non-linear interaction of these stimuli distortion products emerge, with the cubic difference tone ($2f_1 - f_2$) being the most prominent. A very compact representation can be achieved when using the so called *scissor paradigm* [13]. The tone levels of the stimuli are computed according to $L1 = 0.4L2 + 39$ dB. The frequency ratio is fixed with $f_2/f_1 = 1.2$.

Figure 9 shows on the upper panel the distortion product level as a function of the secondary stimulus level $L2$. On the lower panel the corresponding slope is shown. The model is linear for low-level stimuli, hence the initial slope is about 1 dB / dB indicating linear growth. With increasing stimulus level the non-linearity is noticeable, as the slope decreases to about 0.5 dB / dB. The level of the emissions as well as the slope is within those of human measured results shown by Johannesen et al. [14] and Kummer et al. [13]. There are some results of Kummer et al. [13] indicating a non-linear slope for low-level stimuli. Due to the linearity of the model for those amplitudes it is not possible to reproduce this behavior.

To analyze the propagation of the OAE within the cochlea figure 10 shows the decomposition of the involved components for a fixed set of amplitudes plotted along the uncoiled cochlea. The level of the first stimulus is $L1 = 48$ dB SPL and of the second $L2 = 20$ dB SPL. The upper panel shows the magnitude and the lower panel the phase. Alongside the two excitation pattern for the first and second stimulus, the cubic difference tone is shown. The distortion product emerges in the overlapping region of the stimuli (at about 16 mm) indicated by the phase rolling off to base and apex, setting off a new traveling wave wandering to its corresponding characteristic place (at about 20 mm) illustrated by the peak in the magnitude plot.

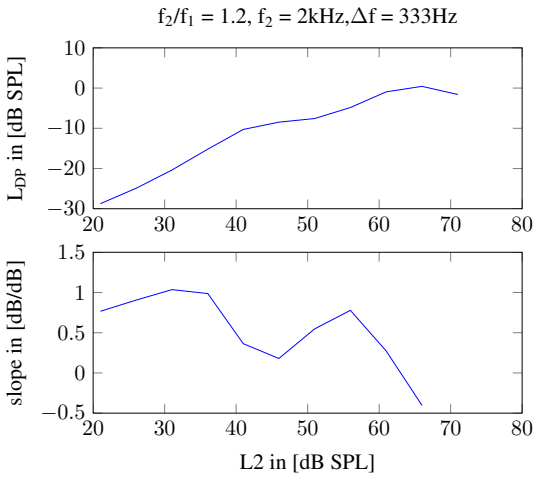

Fig. 9. DPOAE growth of the cubic difference tone as a function of the level $L2$ for a frequency $f_2 = 2$ kHz and a ratio of $f_2/f_1 = 1.2$. The upper panel shows the magnitude of the emission, the lower panel shows the slope.

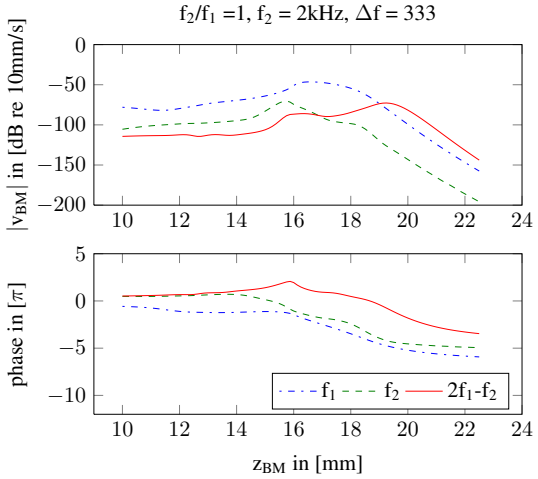

Fig. 10. Illustration of the DPOAE propagation along the cochlea. Magnitude and phase of the interacting stimuli f_1 and f_2 and the emitted cubic difference tone $2f_1 - f_2$ are shown.

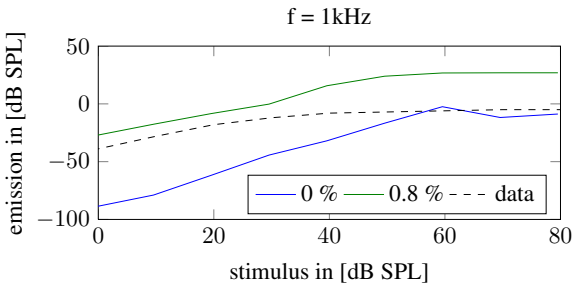

Fig. 11. TEOAE emission sound pressure level simulated in an artificial ear canal as a function of the stimulus level. The results are shown without (0%) and with parameter roughness (0.8%). The dashed line shows the general trend of measured data.

4.2. Transient evoked otoacoustic emissions

Transient evoked otoacoustic emissions (TEOAE) arise when the cochlea is excited with short time stimuli like clicks or tone bursts. Strube [15] estimated parameters for the tone burst leading to an optimal separation of stimulus and emission. For those parameters it was not possible to achieve a reasonable separation as both components overlapped, in consequence we had to shorten the duration for the tonebursts.

Reflections are known to be relevant for the generation of TEOAE [16] but the model parameters show a smooth transition along the cochlea. No major reflection can be expected without any changes to the parameters. Typically biological systems show some irregularities and since reflections have a major impact on TEOAE it is required to take such effects into account. In contrast to Epp et al. [17] not only the basilar membrane stiffness is roughened with a white Gaussian distributed additive term but all relevant parameters of the basilar membrane (w_{BM}, s_{BM}, m_{BM})), Corti resonator (w_{CR}, s_{CR}, m_{CR}) and OHC (K).

Figure 11 shows the resulting emission level as a function of the stimulus level with and without modeled parameter roughness for a Gaussian-modulated pure tone of 1 kHz. To show the general trend of TEOAE measurements, estimated data is shown. Measured data showed to be highly individual, therefore standard reference data is rather sketchy. As expected it is not possible to achieve significant emissions without any roughness and thus below measured results. With 0.8% roughness the low-level emissions are in agreement with measurements, but the for high excitation level the emissions are 10-20 dB above measurements. With such a level of roughness the model is not able to achieve useful results as a frequency analysis tool, due to occurring distortions.

5. Conclusion

The proposed amplification method works as follows: For a sinusoidal excitation of the model with a frequency f, the passive traveling wave wanders across the basilar membrane, where the hair bundles of the OHC along the way are excited. Only within a range where a Corti resonator with a corresponding resonance frequency is excited a reaction can be observed. The amplified traveling wave moves towards its place of resonance, whereas the passive one flats out due to high damping. The Q-factor Q_{CR} defines over which area and the resonance shift in comparison to the basilar membrane resonance R_f where this process takes place.

The time-domain model shows a significant amplification and tuning sharpening as well as maximum shift as known from animal data. At the same time the shift in the resonance frequency is nearly intensity invariant which is consistent with observations of Shera [3]. The decomposition of the altered basilar membrane impedance shows a selective but distinct excitation by the active component. The resulting partial negative real part of the impedance is similar to predictions of de Boer et al. [2]. Despite its simplicity the model is adaptable allowing us to fit the model to measured data. In addition it adjusts smoothly with increasing stimulus level, from active low-level tuning curves with a broad and tall peak to passive damping dominated high-level tuning curves. The corresponding input-output function is realistic as it shows a valid dynamic range and onset of saturation.

The preliminary analysis of the model for OAE data differs. For the DPOAE data it was possible to achieve results similar to human measurements. In addition, the descriptive model approach makes it possible to examine the origin and propagation of the distortion products. The findings support the perspective that the $2f_1 - f_2$ component arises in the overlapping region of the stimuli, setting off a new traveling wave. For some humans measurements indicate a non-linear behavior for low excitation levels. As the model is linear for such levels, it was not possible to reproduce non-linear behavior for stimuli below the onset of the OHC characteristic.

The TEOAE results show a significant discrepancy to measurements. It was not possible to resolve this problem by means of a simple parameter variation. This has to be approached in a future version of PhyBAM with an additional structural enhancement of the model.

6. Acknowledgements

This work is funded by the Deutsche Forschungsgemeinschaft (grant HU 352/10). The authors would like to thank Thorsten Müller and Yashar Bonabi for implementing model parts and helpful discussions.

7. References

[1] H. Hudde and S. Becker, "A physiology-based auditory model elucidating the function of the cochlear amplifier and related phenomena. part i: Model structure and computational method.", ICA 2013 Montreal (2013).

[2] E. de Boer and A. L. Nuttall, "The mechanical waveform of the basilar membrane. ii. from data to models–and back.", J. Acoust. Soc. Am. **107**, 1487–1496 (2000).

[3] C. Shera, "Intensity-invariance of fine time structure in basilar-membrane click responses: Implications for cochlear mechanics", J. Acoust. Soc. Am. **110**, 332–348 (2001).

[4] B. Moore, *Cochlear Hearing Loss: Physiological, Psychological and Technical Issues*, Wiley series in human communication science (Wiley) (2007).

[5] Shamma, S.A., Chadwick, R.S., Wilbur, W.J., Morrish, K.A., Rinzel, J., "A biophysical model of cochlear processing: Intensity dependence of pure tone responses", J. Acoust. Soc. Am. **80**, 133–145 (1986).

[6] J. Santos-Sacchi, "Harmonics of outer hair cell motility.", Biophys. J. **65**, 2217–2227 (1993).

[7] Temchin, A.N., Rich, N. C., Ruggero, M.A., "Threshold tuning curves of chinchilla auditory-nerve fibers. i. dependence on characteristic frequency and relation to the magnitudes of cochlear vibrations", J. Neurophysiol. **100**, 2889–2898 (2008).

[8] P. W. van Hengel, *Comment to paper presented by Shera and Zweig* (edited by H. Duifhuis, J. W. Horst, P. van Dijk, and S. M. van Netten (World Scientific, Singapore)) (1993).

[9] P. Fuchs, *The Oxford Handbook of Auditory Science: The Ear*, volume 1 (2010).

[10] J. B. Allen, "Cochlear micromechanics–a physical model of transduction.", J. Acoust. Soc. Am. **68**, 1660–1670 (1980).

[11] Lu, T.K., Zhak, S., Dallos, P., Sarpeshkar, R., "Fast cochlear amplification with slow outer hair cells", Hear. Res. **214**, 45–67 (2006).

[12] S. T. Neely and D. O. Kim, "A model for active elements in cochlear biomechanics.", J. Acoust. Soc. Am. **79**, 1472–1480 (1986).

[13] P. Kummer, T. Janssen, and W. Arnold, "The level and growth behavior of the 2 f1-f2 distortion product otoacoustic emission and its relationship to auditory sensitivity in normal hearing and cochlear hearing loss.", J. Acoust. Soc. Am. **103**, 3431–3444 (1998).

[14] P. T. Johannesen and E. A. Lopez-Poveda, "Cochlear nonlinearity in normal-hearing subjects as inferred psychophysically and from distortion-product otoacoustic emissions.", J. Acoust. Soc. Am. **124**, 2149–2163 (2008).

[15] H. W. Strube, "Evoked otoacoustic emissions as cochlear bragg reflections", Hear. Res. **38**, 35–45 (1989).

[16] A. Moleti, N. Paternoster, D. Bertaccini, R. Sisto, and F. Sanjust, "Otoacoustic emissions in time-domain solutions of nonlinear non-local cochlear models.", J. Acoust. Soc. Am. **126**, 2425–2436 (2009).

[17] B. Epp, J. L. Verhey, and M. Mauermann, "Modeling cochlear dynamics: interrelation between cochlea mechanics and psychoacoustics.", J. Acoust. Soc. Am. **128**, 1870–1883 (2010).